doi:10.1093/brain/awaa069 BRAIN 2020: 143; 1143–1157 | 1143

BRAIN
A JOURNAL OF NEUROLOGY

Electrographic predictors of successful weaning from anaesthetics in refractory status epilepticus

Daniel B. Rubin,[1,2] Brigid Angelini,[1] Maryum Shoukat,[1] Catherine J. Chu,[1] Sahar F. Zafar,[1] M. Brandon Westover,[1] Sydney S. Cash[1] and Eric S. Rosenthal[1]

See Rüegg and Sutter (doi:10.1093/brain/awaa073) for a scientific commentary on this article.

Intravenous third-line anaesthetic agents are typically titrated in refractory status epilepticus to achieve either seizure suppression or burst suppression on continuous EEG. However, the optimum treatment paradigm is unknown and little data exist to guide the withdrawal of anaesthetics in refractory status epilepticus. Premature withdrawal of anaesthetics risks the recurrence of seizures, whereas the prolonged use of anaesthetics increases the risk of treatment-associated adverse effects. This study sought to measure the accuracy of features of EEG activity during anaesthetic weaning in refractory status epilepticus as predictors of successful weaning from intravenous anaesthetics. We prespecified a successful anaesthetic wean as the discontinuation of intravenous anaesthesia without developing recurrent status epilepticus, and a wean failure as either recurrent status epilepticus or the resumption of anaesthesia for the purpose of treating an EEG pattern concerning for incipient status epilepticus. We evaluated two types of features as predictors of successful weaning: spectral components of the EEG signal, and spatial-correlation-based measures of functional connectivity. The results of these analyses were used to train a classifier to predict wean outcome. Forty-seven consecutive anaesthetic weans (23 successes, 24 failures) were identified from a single-centre cohort of patients admitted with refractory status epilepticus from 2016 to 2019. Spectral components of the EEG revealed no significant differences between successful and unsuccessful weans. Analysis of functional connectivity measures revealed that successful anaesthetic weans were characterized by the emergence of larger, more densely connected, and more highly clustered spatial functional networks, yielding 75.5% (95% confidence interval: 73.1–77.8%) testing accuracy in a bootstrap analysis using a hold-out sample of 20% of data for testing and 74.6% (95% confidence interval 73.2–75.9%) testing accuracy in a secondary external validation cohort, with an area under the curve of 83.3%. Distinct signatures in the spatial networks of functional connectivity emerge during successful anaesthetic liberation in status epilepticus; these findings are absent in patients with anaesthetic wean failure. Identifying features that emerge during successful anaesthetic weaning may allow faster and more successful anaesthetic liberation after refractory status epilepticus.

1 Department of Neurology, Massachusetts General Hospital, Harvard Medical School, Boston, MA, USA
2 Department of Neurology, Brigham and Women's Hospital, Harvard Medical School, Boston, MA, USA

Correspondence to: Daniel B. Rubin MD, PhD
Department of Neurology
Massachusetts General Hospital Neurosciences Intensive Care Unit
55 Fruit Street
Boston, MA 02114, USA
E-mail: drubin4@partners.org

Keywords: status epilepticus; EEG; functional connectivity

Abbreviations: cEEG = continuous EEG; IV-TLA = intravenous third-line anaesthetic; RSE = refractory status epilepticus

Received October 8, 2019. Revised January 7, 2020. Accepted January 27, 2020. Advance access publication April 8, 2020

Introduction

Refractory status epilepticus (RSE) is a state of ongoing or recurrent seizure activity that persists despite treatment with benzodiazepines and first line anti-epileptic drugs (Brophy *et al.*, 2012). Failure to adequately control seizures can result in long-term neurological sequelae or death (Legriel *et al.*, 2010; Kang *et al.*, 2014; Marawar *et al.*, 2018); the mortality of RSE is estimated to be 16–39% (Mayer *et al.*, 2002; Holtkamp *et al.*, 2005; Novy *et al.*, 2010; Rossetti and Lowenstein, 2011). While it is generally accepted that prompt treatment with an intravenous third-line anaesthetic agent (IV-TLA) is an appropriate treatment for RSE (Holtkamp *et al.*, 2003; Brophy *et al.*, 2012; Glauser *et al.*, 2016), the optimum treatment paradigm is unknown (Rossetti and Lowenstein, 2011; Rossetti *et al.*, 2011). Most commonly, intravenous anaesthetics are titrated to achieve either seizure suppression or a burst suppression pattern on EEG (Holtkamp *et al.*, 2003; Rossetti and Lowenstein, 2011; Rossetti *et al.*, 2011; Brophy *et al.*, 2012; Prisco *et al.*, 2020), but few data exist to guide clinicians to the appropriate duration of anaesthetic treatment and timing of anaesthetic weaning. Patients are commonly treated with a continuous infusion of anaesthetics for 24 h or more before attempting an anaesthetic wean, but this duration is arbitrary and many patients may be able to wean sooner (Holtkamp *et al.*, 2003; Rossetti *et al.*, 2004; Das *et al.*, 2019; Muhlhofer *et al.*, 2019). Additionally, periodic and rhythmic EEG patterns on the ictal-interictal continuum may emerge during anaesthetic weaning, prompting resumption of IV-TLA therapy despite their unknown significance (Das *et al.*, 2018).

Substantial morbidity associated with RSE is attributable to the prolonged use of IV-TLA (Kowalski *et al.*, 2012; Hocker *et al.*, 2013; Wijdicks, 2013; Sutter *et al.*, 2014; Marchi *et al.*, 2015; Sutter *et al.*, 2017), and so interventions that could minimize its duration have the potential to improve outcomes (Madzar *et al.*, 2017). Prolonged duration of IV-TLA therapy can expose patients to the risk of ventilator-associated pneumonia (Kang *et al.*, 2014), and IV-TLAs themselves are associated with hypotension, cardiac arrhythmias, hepatotoxicity, and other agent-specific sequelae, such as propofol infusion syndrome (Hocker *et al.*, 2013; Wijdicks, 2013). Periods of prolonged immobility in the intensive care unit also incur the associated risks of deep vein thromboses, deconditioning, and healthcare-associated infections. However, prematurely weaning anaesthetics exposes patients to risks from inadequately treated status epilepticus. Persistent seizure activity and other ictal-interictal continuum EEG patterns have been shown to lead to hyperglycolysis, elevated brain tissue lactate, brain tissue hypoxia, and long-term structural changes in the brain (Vespa *et al.*, 2010, 2016; Claassen *et al.*, 2013; Struck *et al.*, 2016; Marawar *et al.*, 2018), which carry the risk of long-term neurological sequelae. Persistent status epilepticus is also associated with a number of adverse systemic effects including hypoxia, cardiac dysfunction, renal failure, and metabolic derangements (Sutter *et al.*, 2018).

To determine whether quantitative features of continuous EEG (cEEG) could be used to guide anaesthetic treatment for RSE, we performed a series of analyses on cEEG data recorded from patients undergoing weaning of IV-TLA. Two modes of analysis were performed; a frequency-based analysis quantifying the power within different spectral components of the cEEG, and a spatial-correlation-based analysis quantifying the correlation structure of cortical activity. Individual anaesthetic weans were classified as either successful or unsuccessful based on clinical outcome, and both frequency-domain and spatial-domain cEEG features were compared. We hypothesized that successful and unsuccessful anaesthetic weans can be reliably distinguished by a set of quantitative cEEG features that, therefore, could be used to predict the subsequent outcome of an individual anaesthetic wean.

Materials and methods

Patient selection and study design

The study was approved by the local institutional review board and in compliance with STROBE Statement guidelines (von Elm *et al.*, 2007). From a single-centre prospectively collected cohort of patients' continuous cEEG data, we identified a consecutive series of 34 patients diagnosed with RSE between 2016 and 2019 who were treated with at least one IV-TLA. Patients diagnosed with status epilepticus in the setting of cardiac arrest were excluded; all other underlying diagnoses were included (Table 1 and Supplementary Table 1).

Consistent with recommendations to improve the quality of reporting of diagnostic accuracy studies, we followed the Standards for Reporting Diagnostic Accuracy (STARD) (Bossuyt *et al.*, 2015).

Index tests

For this study, the index test included several prespecified frequency-domain and spatial correlation measures of functional connectivity on cEEG. Multiple prior investigations have demonstrated an association between changes in relative alpha power (8–13 Hz) and the alpha-delta ratio and neurological decline in other forms of acute neurological injury including subarachnoid haemorrhage, ischaemic stroke, and post-anoxic coma (Nuwer *et al.*, 1987; Claassen *et al.*, 2004; Wiley *et al.*, 2017; Rosenthal *et al.*, 2018). As such, we prespecified power in the alpha frequency spectrum (8–13 Hz) and the ratio of alpha to delta power as the main frequency-domain cEEG measures from several frequency-specific measures including power in the theta (4–8 Hz) and delta (0.5–4 Hz) frequency spectra. Given that most network statistics are driven by network density, we prespecified network density as the main index test of functional connectivity from a standard battery of spatial correlation measures of functional connectivity (Faust, 2016). In

Table 1 Patient and attempted IV-TLA wean characteristics

Age/Sex	Aetiology	Wean	Anaesthetic	Summary of EEG findings during anaesthetic wean	Outcome
29/F	Anti-NMDAR encephalitis	1	Propofol	Delta background, intermittent GRDA, rare bioccipital SW	Failure
		2	Propofol	Theta/delta background, intermittent GRDA, rare bioccipital SW	Failure
		3	Propofol Pentobarbital Ketamine Midazolam	Delta background, runs of 0.5–1.0 Hz GPDs, bifrontal SW	Failure
		4	Pentobarbital	Theta background, continuous 2.0 Hz GPDs	Failure
		5	Pentobarbital	Theta/delta background, continuous 2.0 Hz GPDs	Failure
		6	Pentobarbital	Delta background, near-continuous 1.0–3.0 Hz GPDs	Success
65/M	Hepatic encephalopathy	7	Propofol	Theta/delta background, 0.5–2.0 Hz multifocal SW	Failure
59/M	Post-traumatic brain injury epilepsy	8	Propofol Midazolam	Theta/delta background, rare LPDs	Success
67/M	Subdural haematoma	9	Propofol	Theta/delta background, diffuse SW, occasional 0.5–3.0 Hz LPDs	Success
85/F	Cryptogenic	10	Propofol	Alpha background, continuous LPDs	Failure
75/M	Subdural haematoma	11	Propofol	Delta background, intermittent generalized SW	Success
71/F	Embolic stroke	12	Propofol	Theta/delta background, near-continuous 0.5–2.0 Hz LPDs	Failure
28/F	Temporal lobe epilepsy	13	Ketamine	Delta background, near-continuous 1.0–2.0 Hz LPDs	Success
78/F	Subdural haematoma	14	Propofol	BSP evolving to theta/delta background, occasional 1.0 Hz LPDs, frequent lateralized SW	Failure
66/F	Septic aneurysmal SAH	15	Propofol	Theta background, near-continuous 0.5–3.0 Hz LPDs	Failure
68/M	Encephalitis	16	Propofol	Delta background, frequent LPDs, abundant lateralized SW	Success
75/F	Subdural haematoma	17	Propofol	Theta/delta background, frequent BiPDs	Failure
72/F	Embolic stroke	18	Propofol Midazolam	BSP evolving into theta/delta background, near-continuous 0.5 Hz GPDs	Failure
		19	Propofol	Theta/delta background, rare GPDs, infrequent multifocal SW	Success
52/F	Idiopathic epilepsy	20	Pentobarbital Ketamine	BSP background, continuous 1.4–3.3 Hz GPDs	Failure
		21	Midazolam Propofol	Alpha background	Success
58/F	Meningioma	22	Propofol	Theta/delta background, occasional lateralized SW	Failure
		23	Propofol	Alpha/theta background, occasional multifocal SW	Success
62/M	Post-traumatic brain injury epilepsy	24	Propofol	Delta background	Success
50/F	Epilepsy, medication non-compliance	25	Propofol Midazolam	Theta/delta background, frequent generalized discharges	Success
77/F	NSCLC metastasis	26	Propofol	Alpha/theta/delta background, intermittent LRDA, intermittent LPDs	Failure
58/F	Hashimoto's encephalopathy	27	Propofol Midazolam	Theta/delta background, occasional 0.5 Hz LPDs	Success
67/F	Encephalitis	28	Propofol	BSP background, intermittent 0.5–1.5 Hz GPDs, BiPDs, and LPDs	Failure
		29	Propofol Midazolam	Delta background, intermittent 0.5–2.0 Hz GPDs, intermittent multifocal SW	Success
66/F	Meningioma	30	Propofol	Theta/delta background, near-continuous 0.5–1.0 Hz LPDs	Failure
		31	Propofol	Theta/delta background, frequent 0.5–2.0 Hz LPDs	Failure
		32	Propofol	Theta/delta background, frequent 0.7–3.0 Hz LPDs, abundant lateralized SW	Success
65/M	Post-stroke epilepsy	33	Propofol	Delta background	Success
62/F	NSCLC metastasis	34	Midazolam Ketamine	Delta background, continuous 0.5–1.5 Hz GPDs and LPDs	Failure
68/M	Glioma	35	Propofol	Theta/delta background, abundant 0.5–1.0 Hz LPDs, occasional lateralized SW	Failure
		36	Propofol	Theta/delta background, abundant 0.5–1.0 Hz LPDs, occasional lateralized SW	Failure
57/M	Hepatic encephalopathy	37	Propofol	Theta/delta background, near-continuous 1.0–2.0 Hz LPDs	Failure
20/F	Epilepsy	38	Propofol	Theta/delta background	Success
57/M	Toxic-metabolic encephalopathy	39	Midazolam	Theta/delta background, frequent 0.5–1.0 Hz LPDs	Success
69/F	Autoimmune encephalitis	40	Propofol	Theta/delta background, intermittent 1.0–2.5 Hz GPDs	Failure
		41	Propofol Midazolam	Alpha/theta/delta background, intermittent 0.5–1.0 Hz GPDs	Failure
66/F	Acute disseminated encephalomyelitis	42	Propofol Midazolam	Theta/delta background, intermittent 0.3–1.0 Hz BiPDs	Success
44/M	Multiple sclerosis	43	Propofol	Delta background, occasional LRDA, frequent multifocal SW	Success
44/M	Alcohol withdrawal	44	Propofol	Alpha background, rare 0.25–0.5 Hz LPDs, rare lateralized SW	Success
48/F	Glioblastoma	45	Propofol	BSP evolving into delta background, near-continuous 0.5–1.0 Hz GRDA	Success
66/M	Intraparenchymal haemorrhage	46	Propofol	BSP evolving into theta background, abundant 0.5–1.0 Hz LPDs	Success
32/M	Epilepsy, medication non-compliance	47	Propofol	Alpha background, occasional 2.0 Hz GRDA	Success

The EEG summary during anesthetic weaning notes the predominant background activity, the presence and quality of any periodic activity, and the presence of quality of any sporadic discharges. For further details, see Supplementary Table 1. BiPDs = bilateral independent periodic discharges; BSP = burst suppressed; GPDs = generalized periodic discharges; GRDA = generalized rhythmic delta activity; LPDs = lateralized periodic discharges; LRDA = lateralized rhythmic delta activity; NSCLC = non-small-cell lung cancer; SAH = subarachnoid haemorrhage; SW = sharp waves.

addition to network density, a standard series of graph-theoretical parameters describing the topology of the functional network were derived: the clustering coefficient, the characteristic path length, the number of independent components, the number of non-trivial components, the size of the largest independent component, the characteristic path length of the largest component, and the clustering coefficient of the largest component (Bullmore and Sporns, 2009).

All cEEG recordings were acquired using a standard 10–20 electrode arrangement at either 256 or 512 Hz using the XLTEK EEG system (Natus Medical Inc.). For the analysis performed, recordings were low-pass filtered at 125 Hz using a third-order Butterworth filter, notch filtered at 60 Hz and 120 Hz to reduce line noise, and referenced to the average.

Each of the index test measures was calculated based on trends of frequency and time-varying maps of the functional connectivity (Fig. 1). We calculated these measures in 1000-ms intervals with 500-ms overlap between intervals. Power within the alpha, theta, and delta bands was normalized relative to the overall power (0.5–20 Hz) in the EEG signal. For the calculation of functional connectivity, within each 1000-ms segment, the signal at each electrode was z-normalized to zero mean and unit variance over the 1000-ms interval. Normalization was performed on the signal from each electrode independently for each patient. A cross-correlogram of the EEG activity was then calculated between all pairs of electrodes using a ±250-ms window of overlap. The peak in the cross-correlogram between each pair of electrodes was identified, and statistically significant peaks in the cross-correlation defined a connection (Kramer *et al.*, 2009; Chu *et al.*, 2012). For each 1000-ms epoch of data, a network of nodes (the EEG electrodes) and edges (the statistically-significant cross-correlations defining the connections between them) was calculated. From each functional connectivity network, the graph theoretical measures described above were calculated. These data were unavailable to the clinical team and the analysis was performed blinded to the clinical data. As a test intended for clinical implementation in real-world conditions, we did not restrict our analysis to data without artefact.

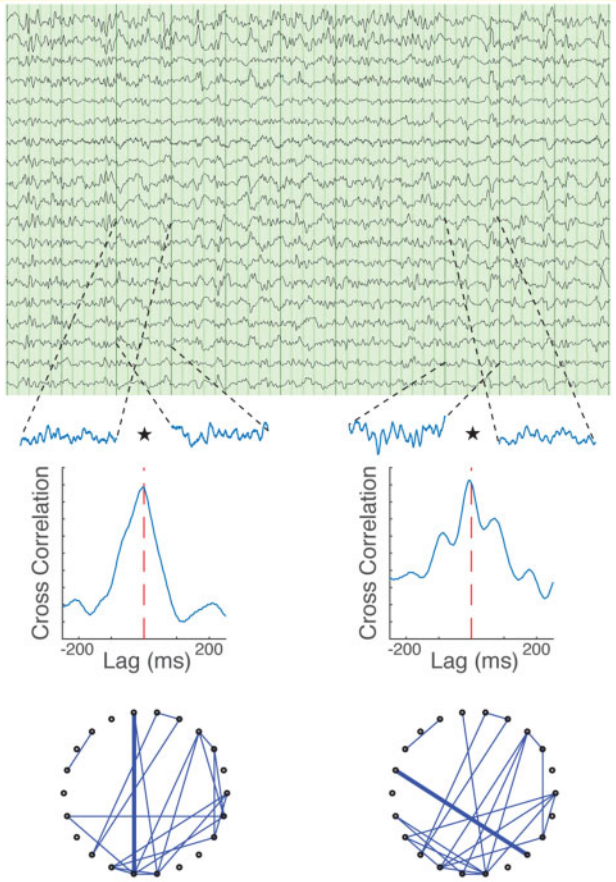

Figure 1 Schematic depicting the calculation of functional connectivity from cEEG. *Top*: An example of 11 s of cEEG data from a patient undergoing an anaesthetic wean. *Middle*: Two pairs of 1-s long EEG tracings are highlighted. The cross correlations between pairs are shown. *Bottom*: Two examples of the functional connectivity maps are shown, with circles (the 'nodes' of the functional connectivity maps) representing each EEG lead and lines (the 'edges' of the functional connectivity maps) representing connections defined by a statistically significant peak in the cross-correlogram between the signals recorded from each lead.

Reference standard clinical outcome

The index test metrics above (alpha power, ratio of alpha to delta power, and network density) were then tested for differences between the reference standard of the successful or failed wean of IV-TLA infusions.

We prespecified both the definition of an attempted wean as well as the definitions of wean success and wean failure through the following systematic process. Medication administration records with time-stamped records of medications, route, concentration, and rate were reviewed. An attempted wean was defined as the cessation of continuous infusion of intravenous anaesthetics. Medical records were then reviewed to confirm that each attempted wean was intended for the purpose of liberating the patient from IV-TLA therapy, as opposed to a temporary pause for a neurological exam. Once confirmed, weans were then classified as either successful or unsuccessful. We defined a successful wean as the cessation of intravenous anaesthetics without the development of recurrent status epilepticus for at least 48 h. We defined an unsuccessful wean as either recurrent status epilepticus or the resumption of intravenous anaesthetics due to clinical or electrographic concern for worsening clinical features on cEEG (e.g. an increase in ictal-interictal continuum burden or frequency). However, the resumption of intravenous anaesthetics specifically for the annotated purpose of patient comfort during intubation was not considered a wean failure. In such cases the wean could either be a success if the patient remained free from recurrent status for 48 h or a failure if recurrent status occurred or anaesthetic therapy was subsequently escalated for the purpose of treating a concerning clinical syndrome or ictal-interictal continuum EEG pattern. Recurrent status epilepticus was defined according to the American Clinical Neurophysiology Society ICU EEG Nomenclature (Hirsch *et al.*, 2013) and International League against Epilepsy (Trinka *et al.*, 2015), including recurrent seizures with evolution and without intervening return to baseline, epileptiform activity with a clinical correlate, or, alternatively, periodic discharges with frequency of 2.5 Hz or greater.

Primary statistical measures

The primary outcome was the differences in spectral power and functional connectivity metrics between successful and unsuccessful weans. Initially, to compare successful and unsuccessful weans, the 30-min period culminating at the time of anaesthesia cessation was identified. The index tests were then averaged over this epoch for each wean. The value of each of these parameters was then compared between successful and failed weans, allowing for no indeterminate test results. To determine whether cEEG preceding these 30-min segments was also predictive at earlier time periods during the wean, we performed the same comparison over the earlier time series for each parameter, specifying time = 0 as the time of cessation of intravenous anaesthetic. The successful and unsuccessful weans were again compared

To measure differences in the index test between wean success and wean failure reference standard outcomes, we measured unpaired two-tailed Student's *t*-test after confirming that parameter sets were adequately normally distributed by a Kolmogorov-Smirnov test of normality. Where direct comparisons of multiple simultaneous parameters were performed, a Holm-Bonferroni procedure was used to correct for multiple comparisons. We considered a corrected *P*-value of <0.05 as statistically significant.

Predictive model: training and testing

We last sought to determine whether the differences described above could be used to train a classifier to predict whether a given anaesthetic wean was likely to be successful based on cEEG characteristics. To do this, we trained a support vector machine using the quantitative parameters calculated above. Two different tests of this model were performed.

A late-epoch prediction model was calculated based on the results of the primary statistical measures during the 30 min preceding the end of each attempted wean. For this 30-min epoch, the calculated quantitative metrics were used to train a support vector machine (SVM) (Cortes and Vapnik, 1995) model using a linear kernel to distinguish between successful and unsuccessful weans. To assess the accuracy of the classifier, a 100-fold cross-validation process was performed. In each iteration, data from 80% of the patients were used to train the classifier and data from 20% of the patients were withheld for testing. The classifier was then used to predict the outcome on the withheld 20% of data, and the accuracy of the classifier was calculated by comparing the predicted outcome to the known outcome in each withheld wean. As a control, a second classifier was trained on the same 80% of the data after randomly shuffling the reference standard outcome measures. This process was repeated 100 times and an average accuracy was calculated for both the true and control classifier. The predictive accuracy of the control model was compared to the model trained on true outcome data.

As an additional test of robustness, the predictive model trained on the primary dataset and validated in the initial hold-out dataset was then used to predict the outcome of anaesthetic weans on an additional validation cohort of 15 anaesthetic weans. This validation cohort was acquired after the performance of the initial analysis and included eight weans (53%) from a second institution. In each of 100 iterations, data from 80% of the patients from the primary dataset were used to train both the classifier and control models. These two models were then used to predict the outcome of 80% of the weans from the validation cohort; again the predictive accuracy of the classifier model and control model was compared.

An early-epoch time-varying prediction model was then developed by applying the classifier to all earlier epochs from each wean, such that the resulting model was applied to the full cEEG record to produce a time-varying 'score' that could be used to predict wean success. The model was again trained using data from the 30-min segments prior to IV-TLA cessation but was then tested at all preceding time points. As in the late-epoch model, on each iteration of a 100-fold cross-validation, weans from 80% of the patients were randomly selected as training data. The trained model was then applied to the full time series data from the withheld 20% of the data, and the prediction accuracy was calculated as a function of time. The model was again compared to a control model trained on randomly shuffled outcome labels.

We finally reported a time-varying 'score' based on the distance from the discrimination boundary in the SVM; a positive score predicts successful weaning based on the current EEG connectivity structure, a negative score predicts wean failure, and the magnitude of the score provides a marker of confidence in the prediction.

Post hoc analysis for oversampling bias

Because some of the patients underwent multiple weans, it is possible that the magnitude of some of the differences we observed were due to within-subject oversampling. To control for this possibility, we repeated the initial analysis comparing the functional connectivity parameters and spectral power between the two groups using only a single wean from each patient.

Data availability

Data are available for review upon request.

Results

Patient and wean characteristics

A total of 47 anaesthetic weans (23 successful, 24 unsuccessful) in 34 patients met criteria for inclusion (Table 1, Supplementary Table 1 and Supplementary Fig. 1) and were included in the primary cohort. The age of the patients ranged from 20 to 85 years old (median age 65); 20 of the 34 patients were female. The causes of status epilepticus in this cohort included autoimmune/paraneoplastic and infectious encephalitides, stroke, subdural haematoma, subarachnoid haemorrhage, metabolic derangement, traumatic brain injury, primary epilepsy syndromes, and primary and metastatic brain tumours. Eight of 34 patients underwent more than one anaesthetic wean; six patients underwent two

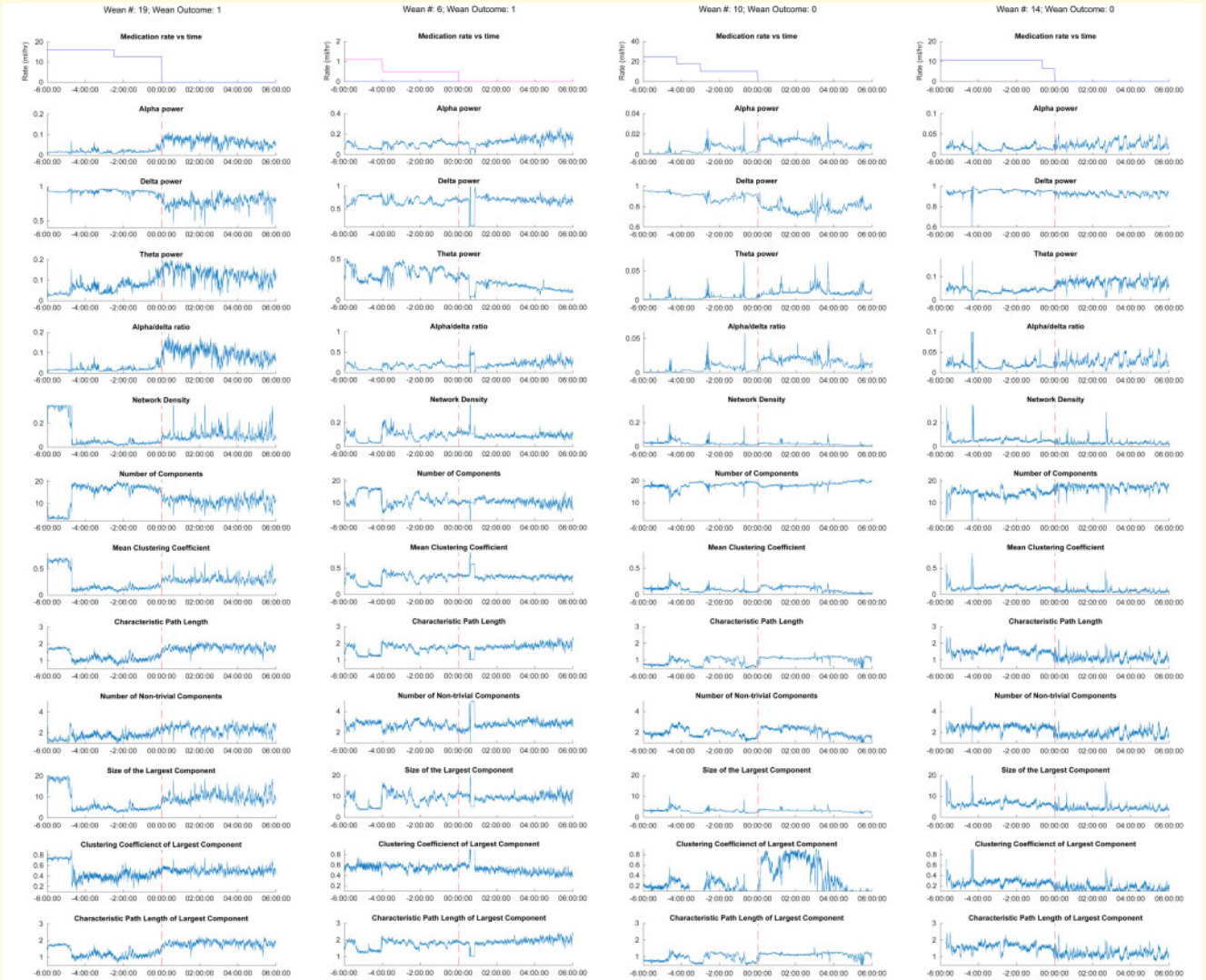

Figure 2 Representative examples of the raw data from patients undergoing successful (*left* column, outcome = 1) and unsuccessful (*right* column, outcome = 0) anaesthetic weans. *Top row*: Intravenous anaesthetic infusion rate versus time. Time = 0 indicates the time of cessation of intravenous anaesthesia. *Rows 2–5*: Frequency-based quantitative metrics (relative alpha power, relative delta power, relative theta power, and alpha/delta ratio) versus time. *Rows 6–13*: Spatial-correlation-based quantitative metrics (network density, number of independent components, mean clustering coefficient, characteristic path length, number of non-trivial components, size of the largest independent component, clustering coefficient of the largest component, and characteristic path length of the largest component) versus time. In both the successful and unsuccessful cases, the alpha/delta ratio rises as intravenous anaesthesia is discontinued. In the successful but not the unsuccessful case, as intravenous anaesthesia is withdrawn, there is a gradual rise in network density, clustering coefficient, characteristic path length, and size of the largest component and fall in the number of independent components as network connectivity rises.

weans, one patient underwent three weans, and one patient underwent six weans. Following conclusion of the primary analysis, a secondary validation cohort of an additional 15 anaesthetic weans (including eight weans from a second institution) was assembled using the same inclusion criteria (Supplementary Table 2).

The most commonly used IV-TLA was propofol (in 40 weans) and the second most frequently used IV-TLA was midazolam (in 11 weans). Pentobarbital was used in five weans and ketamine was used in four weans. Eleven weans involved the use of more than one IV-TLA. Of the 40 anaesthetic weans that included propofol, 20 (50%) were successes and 20 (50%) were failure. Of the seven anaesthetic weans that did not include propofol as one of the IV-TLA, three (43%) were successes and four (57%) were failures. There was no difference in outcome between weans that did and did not include propofol ($P = 1.0$, two-tailed Fisher's exact test). The duration of intravenous anaesthetic weans (measured as the time from peak dose to cessation of infusion) ranged from 1 min (in cases in which anaesthetics were discontinued abruptly) to 69.8 h. The median duration for successful weans was 3.7 h and for unsuccessful weans

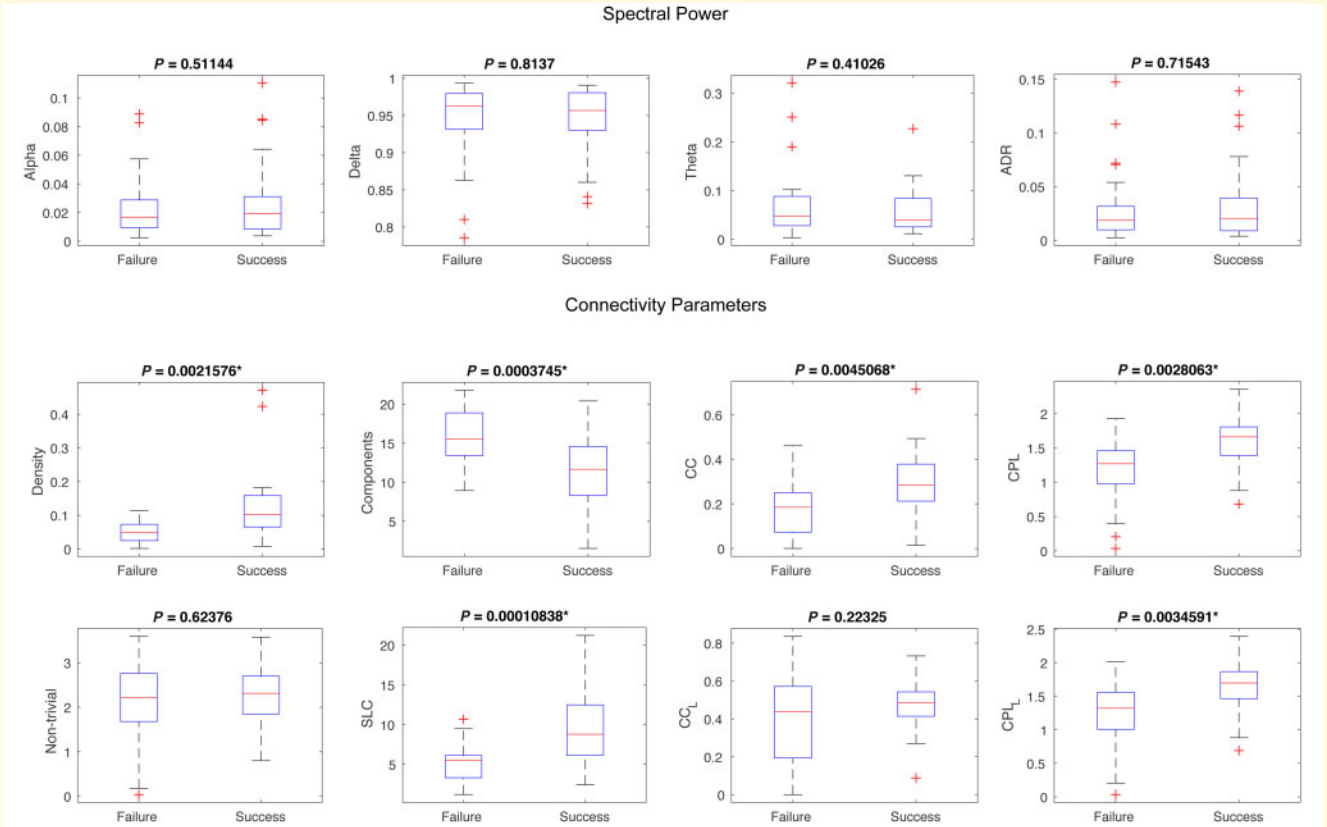

Figure 3 Comparison of the quantitative metrics between successful and unsuccessful anaesthetic weans. Values for each wean are calculated by averaging over the 30-min epoch ending at the time of anaesthesia cessation. *Top row*: There are no significant differences between the two groups in the any of the spectral power metrics. [Alpha: $t(45) = 0.6619$, $P = 0.51144$; Delta: $t(45) = 0.2370$, $P = 0.8137$; Theta: $t(45) = 0.8312$, $P = 0.41026$; ADR: $t(45) = 0.3669$, $P = 0.71543$; two-tailed Student's *t*-test]. *Bottom row*: Compared to the unsuccessful anaesthetic weans, successful anaesthetic weans had significantly greater network density [$t(45) = 3.2549$, $P = 0.0021576$], characteristic path length [$t(45) = 3.1617$, $P = 0.0028063$], clustering coefficient [$t(45) = 2.9903$, $P = 0.0045068$], size of largest component [$t(45) = 4.2437$, $P = 0.00010838$], and characteristic path length of the largest component [$t(45) = 3.0867$, $P = 0.0034591$], and significantly fewer independent components [$t(45) = 3.8467$, $P = 0.0003745$]. There was no significant difference in the number of non-trivial components [$t(45) = 0.4939$, $P = 0.62376$] or the clustering coefficient of the largest component [$t(45) = 1.2350$, $P = 0.22325$]. Within each box plot, the horizontal red line indicates the median value, blue boxes indicate the interquartile range (IQR), and black bars indicate minimum and maximum values (excluding outliers, defined as either >1.5 times the IQR above the third quartile or 1.5 times the IQR below the first quartile, which are indicated by red plus symbol). All *P*-values are calculated by a two-tailed Student's *t*-test; *statistical significance after accounting for multiple comparisons with $\alpha = 0.05$. ADR = alpha/delta ratio; CC = clustering coefficient; CPL = characteristic path length; CC_L and CPL_L = clustering coefficient and characteristic path length of the largest component, respectively; SCL = size of the largest component.

was 3.0 h. There was no significant relationship between wean duration and likelihood of success (U = 264, $P = 0.80$, two-tailed Mann-Whitney U-test). EEG demonstrated a burst-suppression pattern prior to weaning in 18 of the anaesthetic weans, of which seven (39%) were successful. Of those anaesthetic weans that did not follow a period of burst suppression, 16/29 (55%) were successful. There was no difference in outcome between weans that did or did not follow a period of burst suppression ($P = 0.37$, two-tailed Fisher's exact test). The conventional anti-epileptic drugs used varied considerably (Supplementary Table 1); the two most commonly used were levetiracetam (used in 43/47 weans) and phenytoin (used in 32/47 weans).

Examples of the 12 metrics (four frequency-based measures: relative alpha power, relative theta power, relative delta power, and alpha/delta ratio; and eight spatial-correlation-based functional connectivity measures: network density, clustering coefficient, characteristic path length, number of independent components, number of non-trivial components, size of the largest independent component, characteristic path length of the largest component, and clustering coefficient of the largest component) are plotted in Fig. 2 and Supplementary Fig. 2 as time series trends over the course of the wean; the anaesthetic dose is also plotted for reference. Visual inspection of the trends demonstrated several consistent observations. In most cases, the cessation of intravenous

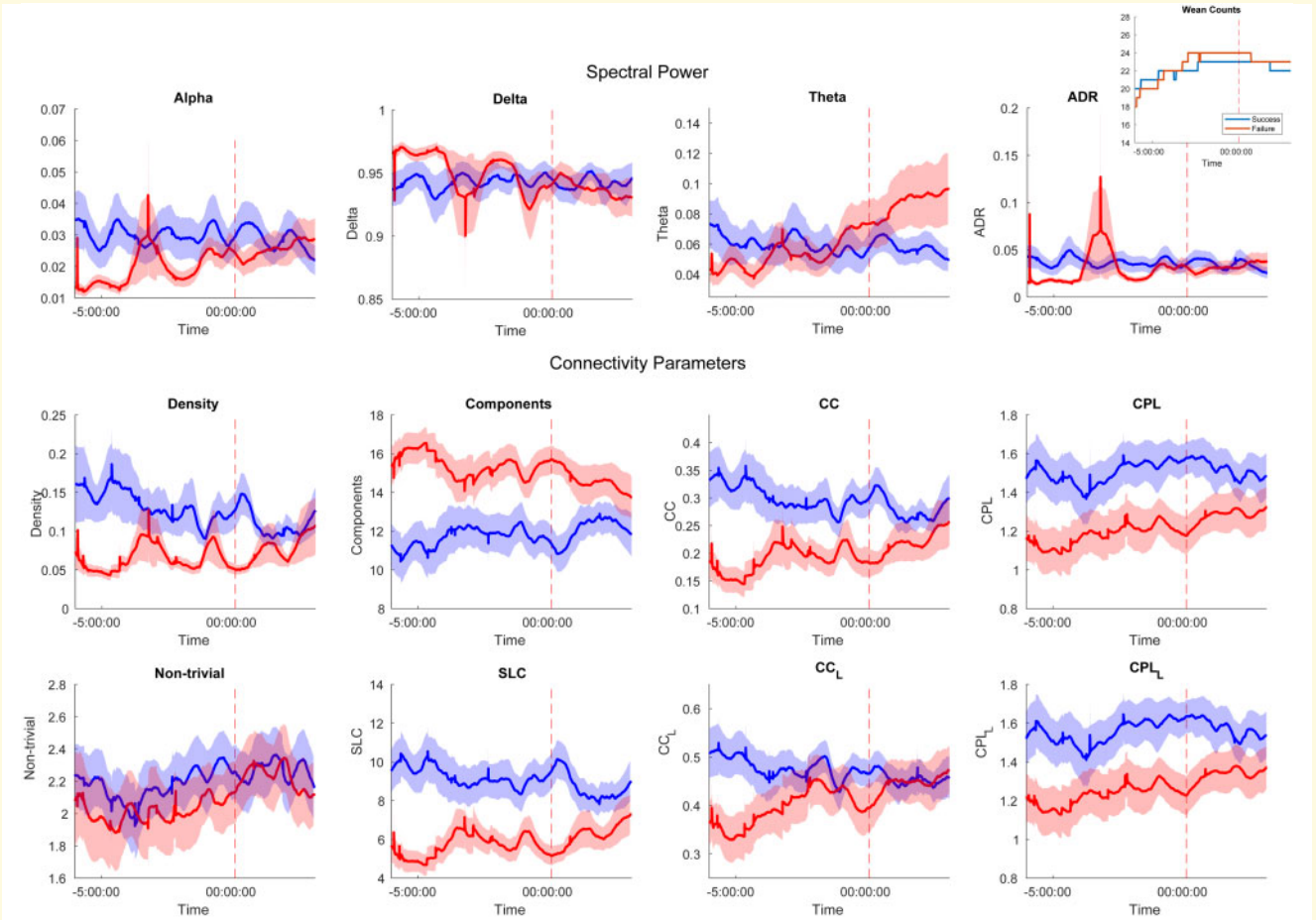

Figure 4 Network connectivity parameters versus time. The four spectral power and eight network connectivity parameters (network density, number of independent components, clustering coefficient, characteristic path length, number of non-trivial components, size of the largest component, clustering coefficient of the largest component, and characteristic path length of the largest component) are plotted for the successful (blue) and unsuccessful (red) weans. Lines indicate mean values, and shaded areas denote the standard error of the mean. The dashed vertical line at time = 0 indicates the time of anaesthesia cessation. EEG data were not available for every anaesthetic wean at all times (in a few cases cEEG was only started 2–3 h prior to anaesthetic weaning); the number of weans included versus time is shown in the *inset*. ADR = alpha/delta ratio; CC = clustering coefficient; CPL = characteristic path length; CC_L and CPL_L = clustering coefficient and characteristic path length of the largest component, respectively; SCL = size of the largest component.

anaesthesia led to a rise in the alpha/delta ratio, regardless of wean outcome. In many of the successful weans, an increase in network density, a decrease in the number of independent components, an increase in the clustering coefficient, and an increase in the size of the largest component were apparent. Overall, the networks appeared to become more spatially connected in these cases. These same changes appeared largely absent from the unsuccessful weans.

Primary statistical outcome measures: comparison of the index test at multiple time points during weaning

Group differences in cEEG index test measures between the wean success and wean failure reference standard outcomes during the 30-min period prior to IV-TLA cessation are reported in Fig. 3. Between the successful and unsuccessful weans, there was no difference in the main frequency-specific outcomes, specifically relative alpha power [$t(45) = 0.6619$, $P = 0.51144$, two-tailed Student's *t*-test] or the ratio of alpha to delta power [$t(45) = 0.3669$, $P = 0.71543$; two-tailed Student's *t*-test]. Additionally, there was no difference in relative delta [$t(45) = 0.2370$, $P = 0.8137$, two-tailed Student's *t*-test] or theta power [$t(45) = 0.8312$, $P = 0.41026$, two-tailed Student's *t*-test]. Given the differential effects of intravenous anaesthetics on EEG power within the beta range, we also compared the power within the $beta_1$ (12.5–16 Hz) and $beta_2$ (16–20 Hz) bands, and similarly found no difference between successful and unsuccessful weans [$beta_1$: $t(45) = 0.1950$, $P = 0.8463$, two-tailed Student's *t*-test; $beta_2$: $t(45) = 0.7625$, $P = 0.4497$, two-tailed Student's *t*-test; Supplementary Fig 3]. In contrast, there was

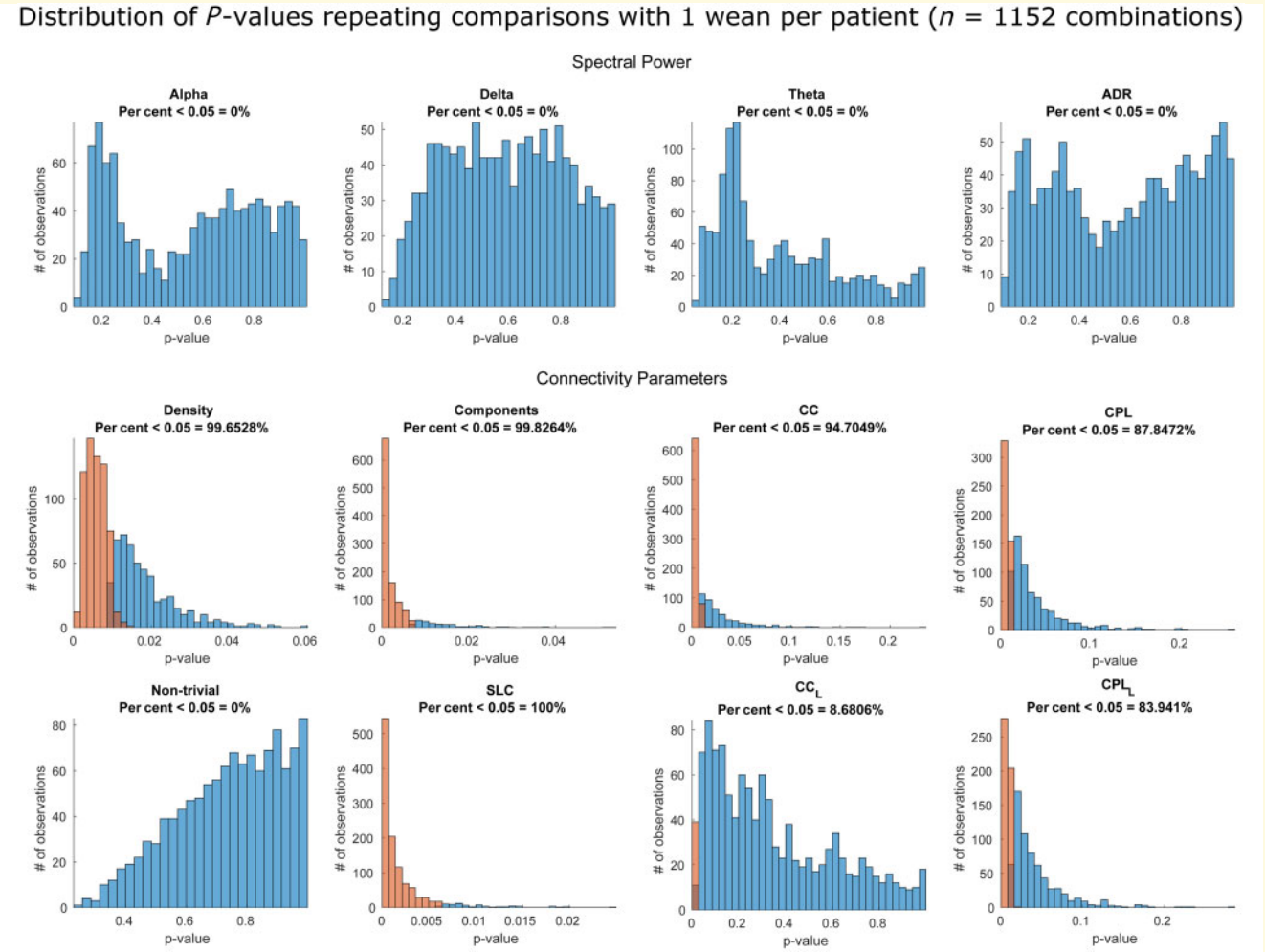

Figure 5 Test of oversampling bias. The comparisons for each quantitative metric was repeated using a single wean from each of the 34 patients; 1152 unique combinations were considered. A histogram of the *P*-values of the differences between the two groups (using a two-sided Student's *t*-test) is shown for each of the four spectral power metrics and each of the eight functional connectivity metrics. Orange bars denote *P*-values that are statistically significant ($\alpha = 0.05$) after accounting for multiple comparisons; blue bars tally the *P*-values that do not reach statistical significance. For the spectral power metrics, in none of the 1152 combinations are any statistically significant differences between the two groups observed. For the six functional connectivity metrics in which a statistically significant difference was observed in the initial analysis (Fig. 3), the majority of the 1152 comparisons yield statistically significant *P*-values. These six histograms skew strongly to the left, indicating that in cases that did not reach statistical significance after correcting for multiple comparisons there was still a trend towards a difference between the groups. ADR = alpha/delta ratio; CC = clustering coefficient; CPL = characteristic path length; CC_L and CPL_L = clustering coefficient and characteristic path length of the largest component, respectively; SCL = size of the largest component.

a difference between the wean success and wean failure groups for the main functional connectivity index test, network density [$t(45) = 3.2549$, $P = 0.0021576$, two-tailed Student's *t*-test]. Overall, there were statistically significant differences for six of the eight parameters that characterize the functional connectivity of the network. Specifically, network density, clustering coefficient [$t(45) = 2.9903$, $P = 0.0045068$, two-tailed Student's *t*-test], characteristic path length [$t(45) = 3.1617$, $P = 0.0028063$, two-tailed Student's *t*-test], size of the largest component [$t(45) = 4.2437$, $P = 0.00010838$, two-tailed Student's *t*-test], and characteristic path length of the largest component [$t(45) = 3.0867$, $P = 0.0034591$, two-tailed Student's *t*-test] were significantly higher during wean success, and the number of independent components was significantly lower [$t(45) = 3.8467$, $P = 0.0003745$, two-tailed Student's *t*-test] during wean success compared with wean failure. There was no significant difference in the number of non-trivial components [$t(45) = 0.4939$, $P = 0.62376$, two-tailed Student's *t*-test] or the clustering coefficient of the largest component [$t(45) = 1.2350$, $P = 0.22325$, two-tailed Student's *t*-test]. As described in the 'Materials and methods' section, a 30-min

time segment was used for these comparisons; however, shorter and longer time periods of comparison yielded similar results (Supplementary Fig. 4).

Group differences in cEEG index test measures between the wean success and wean failure reference standard outcomes during earlier time points is shown in Fig. 4. Because of the multi-hour duration of these cEEG segments, these data contain cEEG segments corrupted by ICU artefacts, and some cEEG records were not available for all time periods. Nonetheless, these data from real-time clinical recordings confirm and extend the findings from the 30-min analysis, demonstrating that up to 6 h prior to discontinuation of anaesthesia, that network density, clustering coefficient, and size of the largest component of the network are consistently greater and that the number of independent components is consistently lower in the wean success group than wean failure group. Interestingly, for some parameters, differences between the reference standard outcome groups are greatest earlier in the wean course.

As burst suppression may have an impact on network density and the subsequently evolution of other network features, we also explored whether there was any difference in network parameters between those anaesthetic weans that did or not follow a period of burst suppression. Similar to our finding that burst suppression did not significantly impact outcome, we saw no significant difference in network features between those anaesthetic weans that did or did not follow a period of burst suppression (Supplementary Fig. 5A) nor any significant difference in network density up to 24 h prior to wean cessation (Supplementary Fig. 5B).

In the *post hoc* analysis for within-subject oversampling bias, we identified eight patients who underwent multiple weans, and a total of 1152 different possible combinations ($6 \times 3 \times 2^6 = 1152$) of weans using only a single wean from each patient. For each combination, the comparison of all 12 metrics was performed, and the *P*-values of the differences between the groups were calculated (Fig. 5). In most cases the differences between the groups persisted. The histograms of the *P*-values were skewed leftward and *P*-values remained <0.05 in the majority cases for the six connectivity parameters in which a difference was noted in the full dataset. In some instances of evaluating a single wean per patient, *P*-values within each outcome group were not small enough to be considered significant after both minimizing the data samples and subsequently correcting for multiple comparisons.

Predictive model accuracy

The late-epoch prediction model developed in the training set could correctly predict the outcome of wean success with 76.4% training accuracy (95% CI: 75.7–77.0) and 75.5% testing accuracy (95% CI: 73.1–77.8%) in the withheld data; the control model with randomly shuffled labels had 45.9% testing accuracy in the withheld data [$\chi^2(1) = 94.5114$, $P = 2.44 \times 10^{-22}$, Kruskal-Wallis H-test] (Fig. 6A). When applied to the second external validation cohort, the

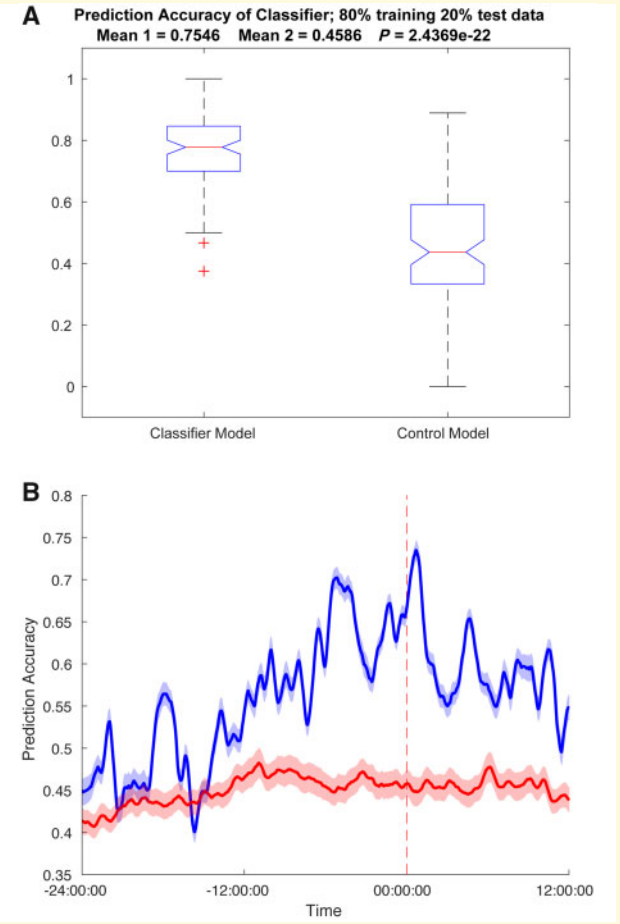

Figure 6 Accuracy of classifier tested by 100-fold cross validation. (**A**) For each of 100 iterations, the classifier was trained on data from a randomly selected 80% of patients, and then tested on the remaining 20% of the data. Data used for training and testing were calculated by averaging the quantitative metrics for each wean over the 30-min period ending at the time of anaesthesia cessation. Results from the true classifier model are shown on the *left*, and from a control model trained on randomly shuffled outcome labels on the *right*. Median accuracy from 100 iterations is indicated by the horizontal red line, blue boxes indicate the IQR of the distribution, and black bars indicate the minimum and maximum values (excluding outliers, defined as either >1.5 times the IQR above the third quartile or 1.5 times the IQR below the first quartile, which are indicated by red plus symbol). The classifier model trained on true outcome labels accurately predicted wean outcome 75.5% of the time, significantly greater than the control model [$\chi^2(1) = 94.5114$, $P = 2.44 \times 10^{-22}$, Kruskal-Wallis H-test]. (**B**) Again, for each of 100 iterations, the classifier was trained on weans from a randomly selected 80% of patients, and then tested on the remaining 20% of the data. Here the model was then applied to the full time series for the withheld 20% of data, yielding a prediction (success versus failure) as a function of time. The accuracy of the model at each time point was calculated for each iteration, and the mean ± standard error of the mean (SEM) of the accuracy is plotted as a function of time. The true classifier model is plotted in blue, and the control model is plotted in red. The two models begin to diverge at ~16 h prior to wean cessation. The classifier is more accurate than the control up to 12 h prior to wean cessation and increases in accuracy over time.

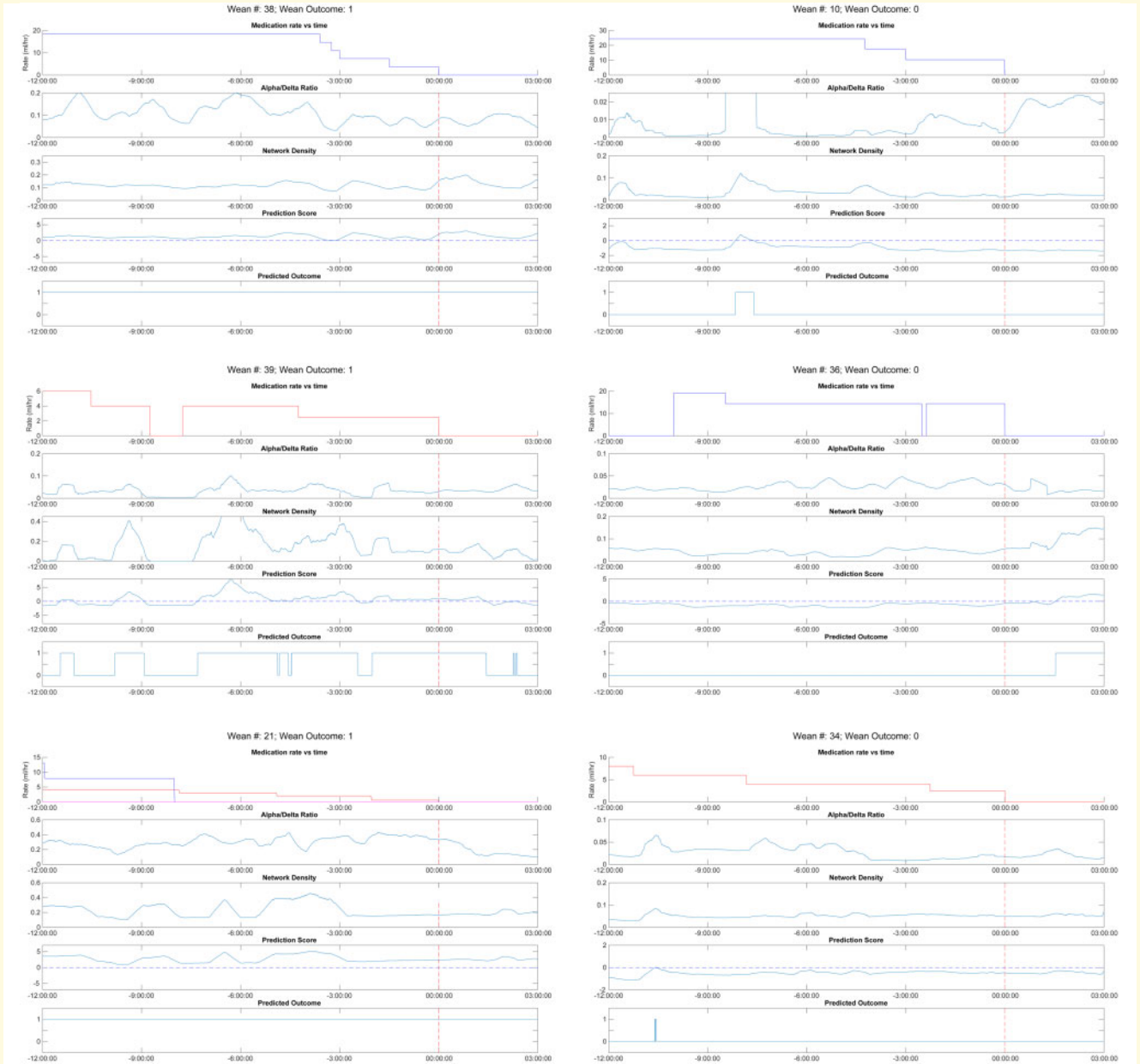

Figure 7 Examples of the classifier applied to time series. For each of six example anaesthetic weans in patients with successful (wean outcome: 1) and unsuccessful anaesthetic liberation (wean outcome: 0): the top parameter is the anaesthetic dose over time. The second and third parameters display the alpha delta ratio and network density over time. The fourth parameter displays the prediction 'score', demonstrating the sign (positive, predictive of success, and negative, predictive of failure) and the confidence of the prediction proportionate to the magnitude of the prediction score. The final parameter demonstrates the time-varying prediction of the wean outcome [success (positive) versus failure (negative) based on the sign of the prediction score].

prediction model had an accuracy of 74.6% (95% CI: 73.2–75.9); the control model with randomly shuffled labels had an accuracy of 47.3% [$\chi^2(1) = 111.9262$, $P = 3.71 \times 10^{-26}$, Kruskal-Wallis H-test]. The area under the curve of the receiver operating characteristic curve was 83.31% in the predictive model and 47.56% in the control model [$\chi^2(1) = 122.0143$, $P = 2.29 \times 10^{-28}$, Kruskal-Wallis H-test] (Supplementary Fig. 6).

The early-epoch time-varying prediction model trained on the reference standard begins to diverge from that of the control model ~16 h prior to wean cessation; by ~12 h prior to wean cessation the prediction model outperforms the

control model and accuracy thereafter improves over time (Fig. 6B). Several examples of the time-varying score are reported in Fig. 7.

Discussion

We found that quantitative cEEG measures of functional connectivity can be used to predict success in weaning from IV-TLA in RSE. Connectivity parameters distinguishing between successful and unsuccessful anaesthetic weans can be detected early in weaning and enable the use of a classifier tool that can predict wean success in a hold-out dataset before the anaesthetic weaning attempt is concluded. The prespecified measure of network density and several associated measures of network connectivity showed good predictive accuracy during multiple time points during anaesthetic weaning. However, no frequency domain measures discriminated wean success from wean failure in this cohort. The model was robust to both a holdout dataset as well as a second validation cohort including data from a second institution.

Though certain clinical characteristics, such as the underlying aetiology of status epilepticus, seizure semiology, and other medical comorbidities all influence the course of treatment in RSE, there is little available evidence to guide decisions regarding the management of IV-TLA, such as the duration of treatment, the rate of weaning, and which IV-TLA agents are weaned first. Earlier awareness that a patient has neurophysiological signatures predicting the successful withdrawal of IV-TLA could lead to earlier liberation from coma and mechanical ventilation.

Prior studies have investigated this question using qualitative assessments of cEEG features during treatment of RSE. Patients in burst suppression while on IV-TLA with epileptiform-appearing bursts are more likely to have recurrent seizures, whereas patients with polymorphic or slow wave bursts are less likely to have recurrent seizure (Johnson *et al.*, 2016; Thompson and Hantus, 2016). Similarly, in patients treated with ketamine for RSE, the resolution of ictal-appearing discharges and the emergence of a medium-voltage theta range activity are predictive of therapeutic response to ketamine and resolution of RSE (Basha *et al.*, 2015). In contrast, a more recent study demonstrated that following cessation of IV-TLA, the emergence of epileptiform appearing activity on the ictal-interictal continuum may not be indicative of wean failure (Das *et al.*, 2018). These conflicting results suggest that qualitative descriptions of EEG morphology during anaesthetic weaning may provide incomplete prognostic information or may be variably and intermittently assessed, highlighting the potential value of a quantitative analysis that offers a consistent, objective, and continuous measurement. Though functional connectivity has been used extensively as an analytic tool within neuroscience to study network dynamics in conditions such as epilepsy (van Mierlo *et al.*, 2014), autism (Matlis *et al.*, 2015), and depression (Kaiser *et al.*, 2016), and other forms of automated cEEG analysis have been used to prognosticate outcome from coma after cardiac arrest (Zubler *et al.*, 2017; Jonas *et al.*, 2019; Kustermann *et al.*, 2019), this is the first study to our knowledge demonstrating the use of functional connectivity to predict outcome and potentially guide treatment in status epilepticus.

We found that successful weaning from intravenous anaesthetics and recovery from RSE is preceded by cortical activity with significantly increased density, fewer independent components, higher clustering coefficients, and larger largest components. Though several of these measures are closely correlated and largely driven by network density (Faust, 2016), overall this pattern suggests that recovery from RSE is associated with more highly correlated cortical activity. Given that seizures are often thought of as a state of pathological hyper-synchrony, this finding may be considered counter-intuitive, but it is consistent with previous work examining changes in functional connectivity in other brain states. Changes in functional network topology over the time course of individual seizures demonstrates that seizure termination is characterized by an increase in functional network density (Schindler *et al.*, 2008; Kramer *et al.*, 2010) and size of the largest component (Kramer *et al.*, 2010) of functional networks, both of which were similarly found to be characteristics of successful anaesthetic weans in the present study. Given consistent observations in these prior studies of functional network changes during the termination of discrete seizures and the present work examining network changes in patients with resolving RSE, we speculate that neuronal network mechanisms of seizure termination may be shared by networks with resolved RSE. Moreover, it may be that network properties that support seizure propagation in the ictal state, when present in the interictal state, may predispose to recurrent seizures and the development of status epilepticus.

There are some important limitations to highlight in this study. While data were prospectively collected and the hypotheses and definitions were pre-specified, the characteristics and dynamics of weans occurred in the clinical setting and were thus uncontrolled, varying across patients and across weans. Although no significant differences were seen in terms of anaesthetic choice or the duration of attempted weans between successful and unsuccessful weans, very abrupt or long-duration weans may have different network physiologies that require validation in a larger and more diverse dataset. Furthermore, the intravenous anaesthetic agents used in this study each have a distinct pharmacokinetic profile that can be further influenced by duration of infusion and patient-specific factors, making it difficult to predict the actual time course of anaesthetic drug levels based on drug infusion rate alone. We attempted to address this potential limitation by specifying wean failure as lack of relapse for 48 h after wean cessation.

A second important potential limitation to this study is the heterogeneity of aetiologies among the patient population. An implicit assumption in the findings described herein is that there is a common physiological mechanism linking status epilepticus caused by different disease processes. However, it is unknown how or if status epilepticus resulting from, for example, subdural haematoma is mechanistically related to status epilepticus resulting from encephalitis. Additional analyses focusing on specific patient populations may be helpful in further clarifying the role of aetiology. Nevertheless, the robustness of the findings across diverse aetiologies suggests that tools derived from this study may be applicable to several different clinical scenarios, which is an inherent strength given the heterogeneity of the neurocritical care population.

Additionally, while we studied quantitative features over visual cEEG interpretation for advantages of reproducibility and continuous performance, there are additional quantitative cEEG metrics that we did not specifically assess in this analysis. Many of these measures, such as spike frequency count, hemispheric asymmetry, focal rhythmicity, autocorrelation, and entropy, may help improve accuracy or better characterize temporal dynamics. Furthermore, the use of other modalities to assess functional connectivity, such as functional MRI or fluoro-deoxyglucose PET (FDG-PET), may provide a powerful insight into the mechanistic implications of the findings described herein. Future efforts to explore additional measures will benefit from the generalizability of the present findings.

While this analysis was performed retrospectively, we envision that such an approach could be applied in the future to develop a real-time analytical tool to be used at the bedside. From a technical standpoint, the computational power necessary to perform the described analyses in real-time is well within capabilities of modern processors. For this study, it took ~2.5 h on a multi-core Linux processor to analyse 24 h of EEG data, demonstrating that the analysis could feasibly run in real-time on an adequately powered system. In our primary analysis, the EEG data were normalized in 1000-ms bins and connectivity analyses averaged over sliding 30-min windows (and as we demonstrate in Supplementary Fig. 4, this time bin can likely be shortened without significantly impacting the results). Once 30-min of EEG data were acquired, a time-varying trend that was updated every 1000 ms could be produced.

Conclusion

RSE yields significant morbidity attributable to the necessary but prolonged use of IV-TLA infusions. We determined that successful weaning from IV-TLA in RSE is heralded by significant changes in the functional connectivity of cortical networks, and that these differences accurately predict anaesthetic liberation at both early and late time points during an attempted anaesthetic wean. These differences may be applied in the ICU to help minimize the duration of pharmacologically induced coma in patients with status epilepticus.

Funding

This work was supported by the National Institutes of Health/National Institute of Neurological Disorders and Stroke (NIH/NINDS) grant R25 NS065743 to D.B.R. He also reports a consultancy with Bristol-Myers Squibb. C.J.C. has consultancies with Biogen, SleepMed, and Alliance Family of Companies. She also receives research support from an NIH/NINDS grant K23 NS092923. S.F.Z. receives research support from SAGE Therapeutics. M.B.W. Received funding from NIH/NINDS K23 NS090900, R01 NS102190, R01 NS102574, R01 NS107291. This work was supported by NIH/NINDS grant R01 NS062092 and NIH/NINDS grant K24 NS088568 to S.S.C. and NIH/NINDS grant K23 NS105950 to E.S.R.

Competing interests

The authors report no competing interests.

Supplementary material

Supplementary material is available at *Brain* online.

References

Basha MM, Alqallaf A, Shah AK. Drug-induced EEG pattern predicts effectiveness of ketamine in treating refractory status epilepticus. Epilepsia 2015; 56: e44–8.

Bossuyt PM, Reitsma JB, Bruns DE, Gatsonis CA, Glasziou PP, Irwig L, et al. STARD 2015: an updated list of essential items for reporting diagnostic accuracy studies. BMJ 2015; 351: h5527.

Brophy GM, Bell R, Claassen J, Alldredge B, Bleck TP, Glauser T, et al. Guidelines for the evaluation and management of status epilepticus. Neurocrit Care 2012; 17: 3–23.

Bullmore E, Sporns O. Complex brain networks: graph theoretical analysis of structural and functional systems. Nat Rev Neurosci 2009; 10: 186–98.

Chu CJ, Kramer MA, Pathmanathan J, Bianchi MT, Westover MB, Wizon L, et al. Emergence of stable functional networks in long-term human electroencephalography. J Neurosci 2012; 32: 2703–13.

Claassen J, Hirsch LJ, Kreiter KT, Du EY, Sander Connolly E, Emerson RG, et al. Quantitative continuous EEG for detecting delayed cerebral ischemia in patients with poor-grade subarachnoid hemorrhage. Clin Neurophysiol 2004; 115: 2699–710.

Claassen J, Perotte A, Albers D, Kleinberg S, Schmidt JM, Tu B, et al. Nonconvulsive seizures after subarachnoid hemorrhage: multimodal detection and outcomes. Ann Neurol 2013; 74: 53–64.

Cortes C, Vapnik V. Support-vector networks. Mach Learn 1995; 20: 273–97.

Das AS, Lee JW, Izzy S, Vaitkevicius H. Ultra-short burst suppression as a 'reset switch' for refractory status epilepticus. Seizure 2019; 64: 41–4.

Das AS, Lee JW, Rosenthal ES, Vaitkevicius H. Successful wean despite emergence of ictal-interictal EEG patterns during the weaning of prolonged burst-suppression therapy for super-refractory status epilepticus. Neurocrit Care 2018; 29: 452–62.

Faust K. Very local structure in social networks. Sociol Methodol 2016; 37: 209–56.

Glauser T, Shinnar S, Gloss D, Alldredge B, Arya R, Bainbridge J, et al. Evidence-based guideline: treatment of convulsive status epilepticus in children and adults: report of the Guideline Committee of the American Epilepsy Society. Epilepsy Curr 2016; 16: 48–61.

Hirsch LJ, LaRoche SM, Gaspard N, Gerard E, Svoronos A, Herman ST, et al. American clinical neurophysiology society's standardized critical care EEG terminology: 2012 version. J Clin Neurophysiol 2013; 30: 1–27.

Hocker SE, Britton JW, Mandrekar JN, Wijdicks EF, Rabinstein AA. Predictors of outcome in refractory status epilepticus. JAMA Neurol 2013; 70: 72–7.

Holtkamp M, Masuhr F, Harms L, Einhaupl KM, Meierkord H, Buchheim K. The management of refractory generalised convulsive and complex partial status epilepticus in three European countries: a survey among epileptologists and critical care neurologists. J Neurol Neurosurg Psychiatry 2003; 74: 1095–9.

Holtkamp M, Othman J, Buchheim K, Meierkord H. Predictors and prognosis of refractory status epilepticus treated in a neurological intensive care unit. J Neurol Neurosurg Psychiatry 2005; 76: 534–9.

Johnson EL, Martinez NC, Ritzl EK. EEG characteristics of successful burst suppression for refractory status epilepticus. Neurocrit Care 2016; 25: 407–14.

Jonas S, Rossetti AO, Oddo M, Jenni S, Favaro P, Zubler F. EEG-based outcome prediction after cardiac arrest with convolutional neural networks: performance and visualization of discriminative features. Hum Brain Mapp 2019; 40: 4606–17.

Kaiser RH, Whitfield-Gabrieli S, Dillon DG, Goer F, Beltzer M, Minkel J, et al. Dynamic resting-state functional connectivity in major depression. Neuropsychopharmacology 2016; 41: 1822–30.

Kang BS, Jhang Y, Kim YS, Moon J, Shin JW, Moon HJ, et al. Etiology and prognosis of non-convulsive status epilepticus. J Clin Neurosci 2014; 21: 1915–9.

Kowalski RG, Ziai WC, Rees RN, Werner JK Jr, Kim G, Goodwin H, et al. Third-line antiepileptic therapy and outcome in status epilepticus: the impact of vasopressor use and prolonged mechanical ventilation. Crit Care Med 2012; 40: 2677–84.

Kramer MA, Eden UT, Cash SS, Kolaczyk ED. Network inference with confidence from multivariate time series. Phys Rev E Stat Nonlin Soft Matter Phys 2009; 79: 061916.

Kramer MA, Eden UT, Kolaczyk ED, Zepeda R, Eskandar EN, Cash SS. Coalescence and fragmentation of cortical networks during focal seizures. J Neurosci 2010; 30: 10076–85.

Kustermann T, Nguepnjo Nguissi NA, Pfeiffer C, Haenggi M, Kurmann R, Zubler F, et al. Electroencephalography-based power spectra allow coma outcome prediction within 24 h of cardiac arrest. Resuscitation 2019; 142: 162–7.

Legriel S, Azoulay E, Resche-Rigon M, Lemiale V, Mourvillier B, Kouatchet A, et al. Functional outcome after convulsive status epilepticus. Crit Care Med 2010; 38: 2295–303.

Madzar D, Knappe RU, Reindl C, Giede-Jeppe A, Sprugel MI, Beuscher V, et al. Factors associated with occurrence and outcome of super-refractory status epilepticus. Seizure 2017; 52: 53–9.

Marawar R, Basha M, Mahulikar A, Desai A, Suchdev K, Shah A. Updates in refractory status epilepticus. Crit Care Res Pract 2018; 2018: 9768949.

Marchi NA, Novy J, Faouzi M, Stahli C, Burnand B, Rossetti AO. Status epilepticus: impact of therapeutic coma on outcome. Crit Care Med 2015; 43: 1003–9.

Matlis S, Boric K, Chu CJ, Kramer MA. Robust disruptions in electroencephalogram cortical oscillations and large-scale functional networks in autism. BMC Neurol 2015; 15: 97.

Mayer SA, Claassen J, Lokin J, Mendelsohn F, Dennis LJ, Fitzsimmons BF. Refractory status epilepticus: frequency, risk factors, and impact on outcome. Arch Neurol 2002; 59: 205–10.

Muhlhofer WG, Layfield S, Lowenstein D, Lin CP, Johnson RD, Saini S, et al. Duration of therapeutic coma and outcome of refractory status epilepticus. Epilepsia 2019; 60: 921–34.

Novy J, Logroscino G, Rossetti AO. Refractory status epilepticus: a prospective observational study. Epilepsia 2010; 51: 251–6.

Nuwer MR, Jordan SE, Ahn SS. Evaluation of stroke using EEG frequency analysis and topographic mapping. Neurology 1987; 37: 1153.

Prisco L, Ganau M, Aurangzeb S, Moswela O, Hallett C, Raby S, et al. A pragmatic approach to intravenous anaesthetics and electroencephalographic endpoints for the treatment of refractory and super-refractory status epilepticus in critical care. Seizure 2020; 75: 153–64.

Rosenthal ES, Biswal S, Zafar SF, O'Connor KL, Bechek S, Shenoy AV, et al. Continuous electroencephalography predicts delayed cerebral ischemia after subarachnoid hemorrhage: a prospective study of diagnostic accuracy. Ann Neurol 2018; 83: 958–69.

Rossetti AO, Lowenstein DH. Management of refractory status epilepticus in adults: still more questions than answers. Lancet Neurol 2011; 10: 922–30.

Rossetti AO, Milligan TA, Vulliemoz S, Michaelides C, Bertschi M, Lee JW. A randomized trial for the treatment of refractory status epilepticus. Neurocrit Care 2011; 14: 4–10.

Rossetti AO, Reichhart MD, Schaller MD, Despland PA, Bogousslavsky J. Propofol treatment of refractory status epilepticus: a study of 31 episodes. Epilepsia 2004; 45: 757–63.

Schindler KA, Bialonski S, Horstmann MT, Elger CE, Lehnertz K. Evolving functional network properties and synchronizability during human epileptic seizures. Chaos 2008; 18: 033119.

Struck AF, Westover MB, Hall LT, Deck GM, Cole AJ, Rosenthal ES. Metabolic correlates of the ictal-interictal continuum: FDG-PET during continuous EEG. Neurocrit Care 2016; 24: 324–31.

Sutter R, De Marchis GM, Semmlack S, Fuhr P, Ruegg S, Marsch S, et al. Anesthetics and outcome in status epilepticus: a matched two-center cohort study. CNS Drugs 2017; 31: 65–74.

Sutter R, Dittrich T, Semmlack S, Ruegg S, Marsch S, Kaplan PW. Acute systemic complications of convulsive status epilepticus-A systematic review. Crit Care Med 2018; 46: 138–45.

Sutter R, Marsch S, Fuhr P, Kaplan PW, Ruegg S. Anesthetic drugs in status epilepticus: risk or rescue? A 6-year cohort study. Neurology 2014; 82: 656–64.

Thompson SA, Hantus S. Highly epileptiform bursts are associated with seizure recurrence. J Clin Neurophysiol 2016; 33: 66–71.

Trinka E, Cock H, Hesdorffer D, Rossetti AO, Scheffer IE, Shinnar S, et al. A definition and classification of status epilepticus–Report of the ILAE Task Force on Classification of Status Epilepticus. Epilepsia 2015; 56: 1515–23.

van Mierlo P, Papadopoulou M, Carrette E, Boon P, Vandenberghe S, Vonck K, et al. Functional brain connectivity from EEG in epilepsy: seizure prediction and epileptogenic focus localization. Prog Neurobiol 2014; 121: 19–35.

Vespa P, Tubi M, Claassen J, Buitrago-Blanco M, McArthur D, Velazquez AG, et al. Metabolic crisis occurs with seizures and periodic discharges after brain trauma. Ann Neurol 2016; 79: 579–90.

Vespa PM, McArthur DL, Xu Y, Eliseo M, Etchepare M, Dinov I, et al. Nonconvulsive seizures after traumatic brain injury are associated with hippocampal atrophy. Neurology 2010; 75: 792–8.

von Elm E, Altman DG, Egger M, Pocock SJ, Gøtzsche PC, Vandenbroucke JP. The Strengthening the Reporting of Observational Studies in Epidemiology (STROBE) statement: guidelines for reporting observational studies. Lancet 2007; 370: 1453–7.

Wijdicks EF. The multifaceted care of status epilepticus. Epilepsia 2013; 54 Suppl 6: 61–3.

Wiley SL, Razavi B, Krishnamohan P, Mlynash M, Eyngorn I, Meador KJ, et al. Quantitative EEG metrics differ between outcome groups and change over the first 72 h in comatose cardiac arrest patients. Neurocrit Care 2017; 28: 51–9.

Zubler F, Steimer A, Kurmann R, Bandarabadi M, Novy J, Gast H, et al. EEG synchronization measures are early outcome predictors in comatose patients after cardiac arrest. Clin Neurophysiol 2017; 128: 635–42.